Study on Randomly-Coupled Multi-Core Unit Grouping Fibers

Zhilu Luo[1], Jiajing Tu[1*], Yongneng Jiang[1], Weiping Liu[1], Zhaohui Li[2,3]
[1]Department of Electronic Engineering, School of Information Science and Technology, Jinan University, Guangzhou 510632, China
[2]School of Electronics and Information Technology, Guangdong Provincial Key Laboratory of Optoelectronic Information Processing Chips and Systems, Sun Yat-sen University, Guangzhou, China.
[3]Southern Marine Science and Engineering Guangdong Laboratory (Zhuhai), Zhuhai 519000, China
*Corresponding author: tujiajing@jnu.edu.cn

***Abstract*—We combine the weakly-coupled and strongly-coupled multi-core fiber (MCF) technologies, and propose a new type of randomly-coupled multi-core unit grouping fiber with small group delay spread (GDS). By discussing the core groups arrangement, we give the optimal design scheme.**

Keywords—optical fibers, space-division multiplexing

I. Introduction

Space division multiplexing (SDM) is a candidate to break the capacity limit of traditional single mode fiber [1]. Many types of optical fibers based on SDM transmission are proposed. According to the coupling extent of each core channel, SDM fibers can be divided into uncoupled MCFs and coupled MCFs [2]. Uncoupled MCFs require low crosstalk (XT) between adjacent cores, because each core is used as an individual waveguide. On the other hands, the coupled MCF, namely the randomly coupled MCF takes advantage of multiple-input multiple-out (MIMO) digital signal processing (DSP) technology to compensate the XT, and it can achieve higher spatial channel density than uncoupled-core MCFs [3]. Besides, the randomly-coupled MCF is also conducive to the suppression of GDS and mode-dependent loss (MDL) [4], thus it is suitable for the long-distance transmission.

In this study, we combine the uncoupled and coupled MCF technologies together. As independent elements, several coupled MCFs are deployed in the cladding. Each coupled MCF element, to some extent, can be treated as strongly-couple few-mode core. However, the GDS of the pulse response envelope can be well suppressed and present the linear relationship with square root of transmission distance. In order to keep small MIMO complexity, we fix the core number of the coupled MCF element as 2 and in this case MIMO is fixed at 4×4. We first simulate the core pitch of the coupled two-core element with the lowest GDS. Secondly, we investigate the dependence of crosstalk on the relative angle between the coupled two-core groups, and investigate the crosstalk characteristics of the coupled fiber with different structures.

II. Design of two-core element

The core of the randomly-coupled MCF in this work is a single-mode structure, which should meet the requirement that normalized frequency is smaller than 2.405. Therefore, we set the relative refractive index between the core and the cladding at 0.35% and core radius at 4.5μm. The core pitch (Λ) within the coupled two-core group shown in Fig. 1 should be selected appropriately, because it has large effect on the coupling degree between the super modes generated by the coupled

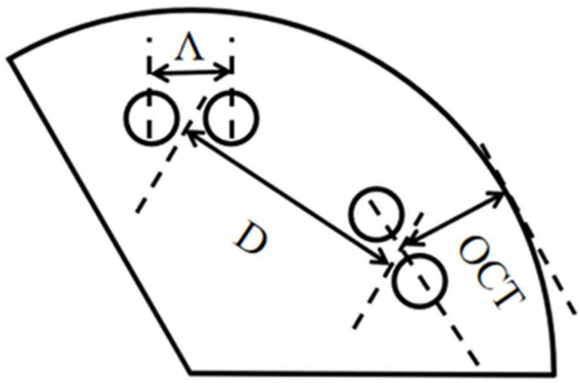

Fig. 1. Partial view of randomly-coupled multi-core unit grouping fiber

cores, which will determine the GDS value. The GDS, σ_{gd} can be calculated by [5]

$$\sigma_{gd}^2 = \frac{1}{N}\left\langle \sum_{i=1}^{N} \tau_i^2 \right\rangle, \tag{1}$$

where N is the number of modes that include the polarizations, and τ_i is the i-th eigenvalues of the group-delay operator (GDO). The GDO is defined as [6]

$$\mathbf{GDO}(\omega) = j\mathbf{T}(\omega)^{-1}\frac{d\mathbf{T}(\omega)}{d\omega}, \tag{2}$$

where $\mathbf{T}$ is the total transmission matrix, and ω is the angular frequency of light. Here, $\mathbf{T}$ was calculated as

$$\mathbf{T} = \prod_{i=1}^{M} \mathbf{T}_i, \tag{3}$$

where $\mathbf{T}_i$ is the i-th transmission matrix of M segments. $\mathbf{T}_i$ is given by the product of the propagation matrix $\mathbf{U}_i$ and the polarization mode rotation matrix $\mathbf{R}_i$. $\mathbf{U}_i$ is the propagation matrix of the i-th segment and block diagonal, so x and y polarizations do not couple within the segment [7]. $\mathbf{R}_i$ represents the effect of rotation between segments caused by twist on the electric field polarization [7]. The bend radius R_b in the calculation was set to be 14 cm. In this calculation, we assumed the fiber twist consists of a non-random component which is a sinusoidally modulated bidirectional twist and a random component with mean value of 0 turn/m and variance of 0.02 turn/m. The final GDS was obtained by averaging 30 instances with the twist condition at the wavelength of 1550 nm.

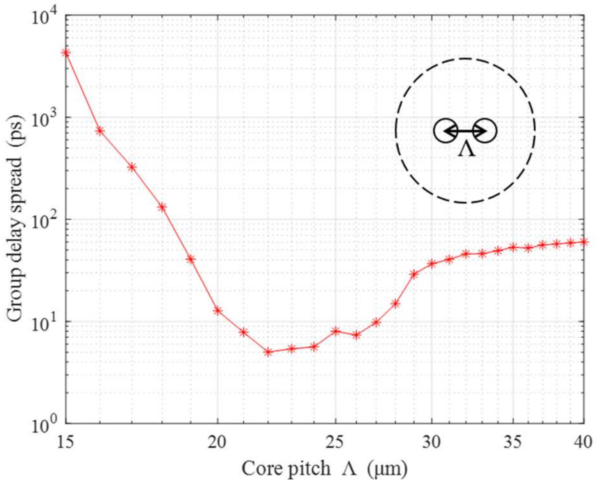

Fig. 2. The simulated relationship between the core pitch and GDS.

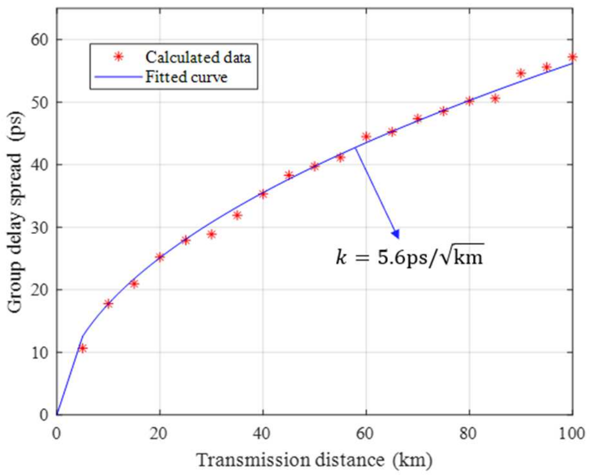

Fig. 3. The simulated relationship between the transmission distance and GDS.

Fig. 2 shows the calculated GDS as a function of the core pitch at a distance of 1 km. The GDS is large for both large and small core pitch, and the GDS is minimum when the core pitch is 22 μm. Therefore, the inner core pitch of coupled two-core groups is set at 24μm in order to obtain the optimal GDS. As shown in Fig. 3, we obtained the spatial mode dispersion (SMD) coefficient, k, of 5.6 ps/√km.

III. Rotation Analysis of the Coupled Two-Core Groups

We use the power coupling theory to calculate the XT between the coupled two-core groups. The power-coupling coefficient (h) was calculated as [8]

$$h_{pq}(z) = \frac{2\bar{\kappa}_{pq} d}{1+\left(\Delta\beta'_{pq} d\right)^2}, \tag{4}$$

where p, q represent core group p and core group q; $\bar{\kappa}_{pq}$ is the average value of κ_{pq} and κ_{qp}; $\Delta\beta'_{pq}$ is the difference of equivalent propagation constant between the coupled two-core groups; d is correlation length, and we assumed that is 0.05m [10]. And the XT with length L was calculated as [10]

$$XT = \tanh\left(\bar{h}_{pq} L\right). \tag{5}$$

In Fig. 4(a), the initial state is when θ_p and θ_q equal 0 degree. For the randomly-coupled MCFs with two-core groups, the two-core group rotates 180 degrees in one cycle. In Fig. 4(b) and Fig. 4(c), the x axis represents θ_p, the y axis represents θ_q, and the z axis represents XT between the two-core groups. The XT of the first and second modes shows a similar trend of change. As shown in Fig. 4(b) and Fig. 4(c), when θ_p and θ_q change to 90 degrees, namely (θ_p, θ_q) tends to (90, 90), the energy overlap between the core groups decreases and the XT between the core groups gradually decreases. When θ_p is 0 degree (or 180 degrees) and θ_q is 0 degree (or 180 degrees), the energy overlap between core groups is the strongest, and the XT between two-core groups reaches the maximum. Moreover, it is observed that the XT of the second mode is higher than that of the first mode.

IV. Arrangement Strategy of the Coupled Two-Core Groups

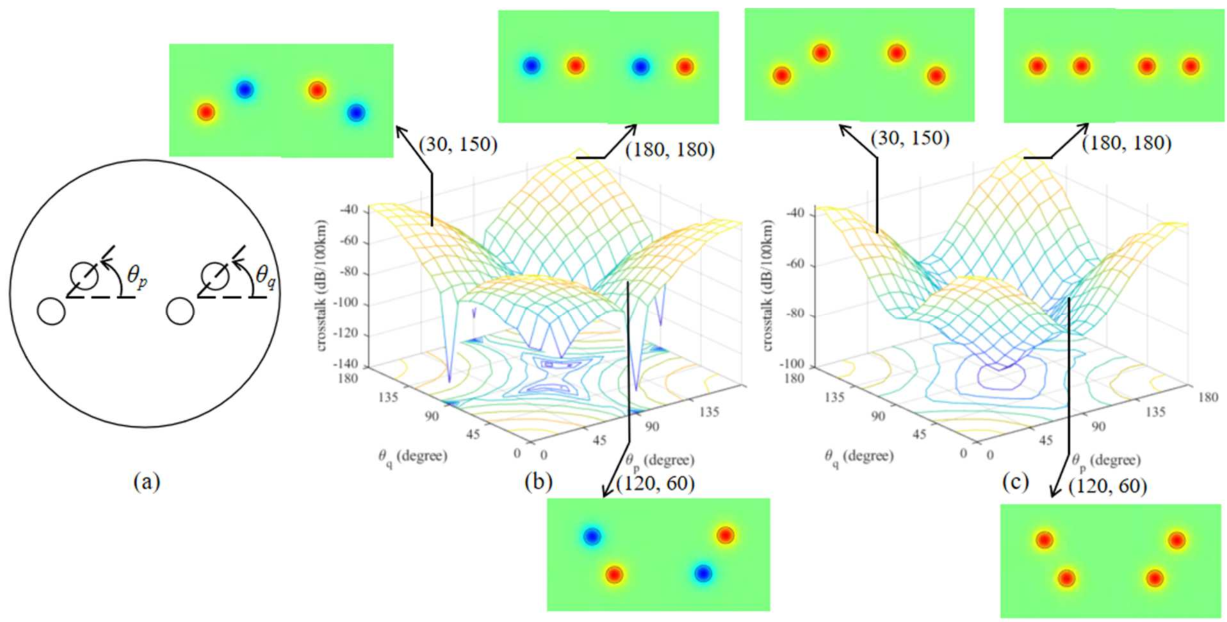

Fig. 1. (a) Schematic illustration of core group rotation (b) The dependence of the second mode crosstalk on rotation angle (c) The dependence of the first mode crosstalk on rotation angle.

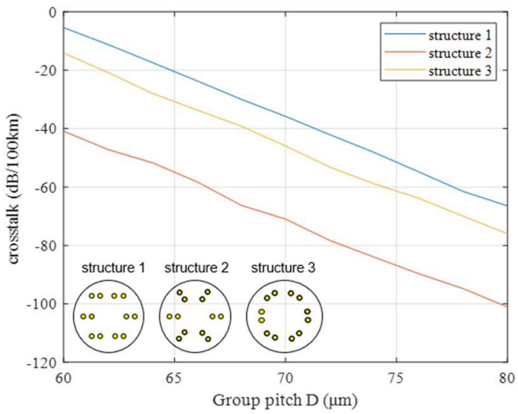

Fig. 4. The simulated relationship between the bending loss and OCT.

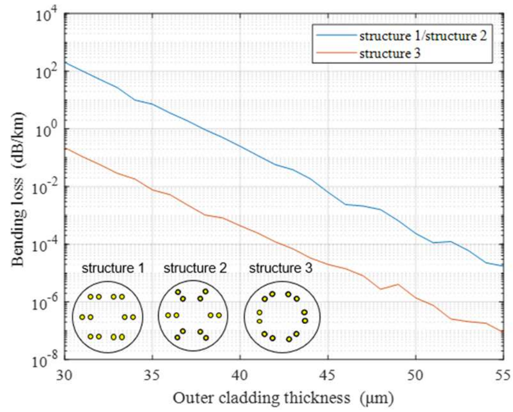

Fig. 5. The simulated relationship between the XT and group pitch.

TABLE I. RARAMETERS OF THREE STRUCTURES OF MCFS

	Structure 1	Structure 2	Structure 3
OCT (μm)	48.5	48.5	38
Group pitch D (μm)	64	64	74.5
XT (dB/100km)	−18	−52	−60

In order to further explore the arrangement of coupled two-core groups, the characteristics of bending loss and the XT between core groups of three types of MCFs with 12 cores arranged in 6 groups of 2 cores are compared.

The results shown in Fig. 5 illustrate the bending loss of structure 1 and structure 2 is obviously greater than that of structure 3. This is because the core arrangements of structure 1 and structure 2 make the core closer to the cladding due to the same outer cladding thickness (OCT).

In addition, it can be observed that the core group arrangement of structure 1 causes θ_p to be 0 degree (or 180 degrees) and θ_q to be 0 degree (or 180 degrees) in adjacent core groups, while the core group arrangement of structure 2 makes the relative rotation angles θ_p and θ_q closer to 90 degrees compared with structure 3. According to Fig. 4(c), the worst crosstalk between core groups of structure 1 is the largest, and structure 2 has minimal the worst crosstalk between core groups.

If the cladding diameter is fixed at 225μm [11] and the requirement of the bending loss is set at 0.001dB/km [12], the parameters of three types of MCFs shown in Table 1. This result indicates that although the crosstalk of structure 2 shown in Fig. 6 is smaller than that of the other two structures, the small OCT of structure 3 makes it reach the lowest level of crosstalk among the three structures.

CONCLUSION

We set the core pitch within the randomly coupled MCF to 22 μm by calculating the GDS, and obtained the SMD coefficient of 5.6 ps/√km. Furthermore, we investigate the dependence of XT between the coupled two-core groups on the two-core group rotation angle. The results show that the XT between two-core groups decreases gradually as θ_p and θ_q approaches 90 degrees. We also discuss the XT characteristics of random coupled MCFs with different structures under the upper limit of the clad diameters of 225μm. It is demonstrated that under the same constraint conditions, the MCF of structure 3 can obtain lower crosstalk than the other two structures, which is about −60 dB/100km.

ACKNOWLEDGMENT

This research was sponsored by Key Technologies Research and Development Program (2021YFB2800901); National Natural Science Foundation of China (U2001601); Guangzhou basic and applied basic research foundation (202002030327); Innovation Group Project of Southern Marine Science and Engineering Guangdong Laboratory (Zhuhai) (SML2022007); Guangdong Basic and Applied Basic Research Foundation No. 2023A1515012984.

REFERENCES

[1] T. Morioka, Y. Awaji, R. Ryf, P. Winzer, D. Richardson and F. Poletti, "Enhancing optical communications with brand new fibers," in IEEE Communications Magazine, vol. 50, pp. s31-s42, Feb. 2012.

[2] K. Saitoh, "Multi-Core Fiber Technology for SDM: Coupling Mechanisms and Design," in Journal of Lightwave Technology, vol. 40, pp. 1527-1543, 1 March 2022,

[3] T. Sakamoto, et al. "Twisting-Rate-Controlled 125 μm Cladding Randomly Coupled Single-Mode 12-Core Fiber," in Journal of Lightwave Technology, vol. 36, pp. 325-330, 15 Jan. 2018.

[4] C. Antonelli, A. Mecozzi, M. Shtaif, N. K. Fontaine, H. Chen and R. Ryf, "Stokes-Space Analysis of Modal Dispersion of SDM Fibers With Mode-Dependent Loss: Theory and Experiments," in Journal of Lightwave Technology, vol. 38, pp. 1668-1677, 1 April 2020,

[5] T. Fujisawa and K. Saitoh, "Group delay spread analysis of strongly coupled 3-core fibers: an effect of bending and twisting," Optics Express, vol. 24, pp.9583-9591, May 2016.

[6] S. Fan and J. M. Kahn, "Principal modes in multimode waveguides," Opt. Lett. vol. 30, pp. 135-137, Jan. 2005.

[7] M. B. Shemirani, W. Mao, R. A. Panicker and J. M. Kahn, "Principal Modes in Graded-Index Multimode Fiber in Presence of Spatial- and Polarization-Mode Coupling," in Journal of Lightwave Technology, vol. 27, pp. 1248-1261, May 2009.

[8] M. Koshiba, K. Saitoh, K. Takenaga and S. Matsuo, "Multi-core fiber design and analysis: coupled-mode theory and coupled-power theory." Opt. Express, vol. 19, pp. B102-B111, 2011.

[9] R. -J. Essiambre, G. Kramer, P. J. Winzer, G. J. Foschini and B. Goebel, "Capacity Limits of Optical Fiber Networks," in Journal of Lightwave Technology, vol. 28, pp. 662-701, Feb. 2010.

[10] J. Tu, K. Saitoh, M. Koshiba, K. Takenaga and S. Matsuo, "Optimized design method for bend-insensitive heterogeneous trench-assisted multi-core fiber with ultra-low crosstalk and high core density," in Journal of Lightwave Technology, vol. 31, pp. 2590-2598, Aug. 2013.

[11] S. Matsuo, et al. "Large-effective-area ten-core fiber with cladding diameter of about 200 μm," Optics Letters, vol. 36, pp. 4626-4628, Dec. 2011.

[12] K. Takenaga, et al. "A large effective area multi-core fiber with an optimized cladding thickness," Opt. Express, vol. 19, pp. B543-B550, July 2011